# Hard X-ray stereographic microscopy for single-shot differential phase imaging

VALERIO BELLUCCI[1], MARIE-CHRISTINE ZDORA[2,3], LADISLAV MIKEŠ[1], SARLOTA BIRNSTEINOVA[1], PETER OBERTA[4,5], MARCO ROMAGNONI[6], ANDREA MAZZOLARI[6], PABLO VILLANUEVA-PEREZ[7], RAJMUND MOKSO[8], CHRISTIAN DAVID[2], MIKAKO MAKITA[1], SILVIA CIPICCIA[9,10], JOZEF ULIČNÝ[11], ALKE MEENTS[12], ADRIAN P. MANCUSO[1,13], HENRY N. CHAPMAN[12], AND PATRIK VAGOVIČ[12,1,*]

[1] *European XFEL, Holzkoppel 4, 22869 Schenefeld, Germany*
[2] *Paul Scherrer Institute, Forschungsstrasse 111, 5232 Villigen PSI, Switzerland*
[3] *Institute for Biomedical Engineering, ETH Zürich, 8092 Zurich, Switzerland*
[4] *Institute of Physics, Academy of Sciences of the Czech Republic v.v.i., Na Slovance 2, 182 21, Praha 8, Czech Republic*
[5] *Rigaku Innovative Technologies Europe s.r.o., Novodvorská 994, 142 21, Praha 4, Czech*
[6] *INFN Sezione di Ferrara, Via Saragat 1, 44122 Ferrara, Italy*
[7] *Synchrotron Radiation Research and NanoLund, Lund University, Box 118, 221 00, Lund, Sweden*
[8] *DTU Physics, Fysikvej, 310, 028 2800 Kgs. Lyngby Denmark*
[9] *Diamond Light Source, Harwell Science and Innovation Campus, Didcot, Oxfordshire OX11 0DE, UK*
[10] *Department of Medical Physics and Biomedical Engineering, University College London, Gower Street, London WC1E 6BT, United Kingdom*
[11] *Faculty of Science, Department of Biophysics, P. J. Šafárik University, Jesenná 5, 04154 Košice, Slovakia*
[12] *Center for Free-Electron Laser Science CFEL, Deutsches Elektronen-Synchrotron DESY, Notkestr. 85, 22607 Hamburg, Germany*
[13] *Department of Chemistry and Physics, La Trobe Institute for Molecular Science, La Trobe University, Melbourne, Victoria 3086, Australia*
[*] *Corresponding author: patrik.vagovic@cfel.de*

*Compiled March 21, 2022*

**The characterisation of fast phenomena, exhibiting velocities of metres per second and more, occurring in opaque samples requires adequate X-ray imaging methods for revealing such structures in their natural state. Fast processes are often stochastic in nature and occur in many key technologies such as additive manufacturing or micro-fluidics, e.g. turbulent cavitations or shock-wave propagation. Due to the complexity of such structures and the speed of the dynamic processes involved, it is necessary to collect 3D structural information for each relevant point in time. Sensitivity to small density differences in a sample can be greatly enhanced, especially for soft matter, by exploiting the phase-contrast modality. In this work, we demonstrate a combination of X-ray stereography and differential phase contrast microscopy with a single-shot (i.e. single exposure) acquisition, paving the way to 3D movies by using sequential "shots" to each collect 3D information. We show that we can successfully recover the 3D phase volume of a phantom object using two simultaneously recorded, stereographic X-ray views. The proposed method is extendable to more than two angular projections and has great potential for applications at megahertz X-ray Free Electron Lasers (XFELs), where velocities of up to kilometres per second can be temporally resolved.** 

http://dx.doi.org/10.1364/ao.XX.XXXXXX

Multi-projection X-ray microscopy methods provide important technological advancements for the visualisation of fast stochastic processes. Samples can be statically placed into the X-ray probes and volume information can be obtained by simultaneous multi-projection (so called "single-shot") acquisition without the need for scanning. In the hard X-ray regime, obtaining multiple projections simultaneously can be achieved by employing crystal beam splitters. These optical elements split the primary beam and generate multiple probes at different angles. When the sample is inserted into the beam just downstream of the splitter, it is illuminated from multiple different directions, providing access to 3D information from a single-shot exposure. Recently, various beam-splitting schemes working with monochromatic or broad band X-ray beams have been proposed and experimentally demonstrated at synchrotrons using Laue or Bragg geometry to generate multiple simultaneous X-ray probes [1–4]. Such approaches enable the simultaneous exposure of multiple angular projections, for example, by a single pulse at XFEL sources. The use of megahertz XFEL sources opens up the possibility of breaking the current technological recording speed barrier of standard tomographic methods, where the world record of tomographic frames per second (tfps) reported so far is 208 [5]. Further increase of tfps is not only challenging from the technological point of view but also affects the dynamics of the samples due to the strong centrifugal forces induced by fast sample rotation. Therefore, the kHz up to MHz sampling regime is not accessible by standard X-ray computed

tomography. The contrast mechanism commonly used in X-ray multi-projection imaging to date is predominantly propagation-based full-field X-ray microscopy based on Fresnel diffraction. It is sensitive to sharp transitions in density, e.g. at the object boundaries, which are consequently rendered with high contrast. However, propagation-based phase contrast is not very sensitive to smooth density variations in a sample. In many fast processes, such as shock wave propagation or mixing of the fluids, smooth density gradients propagating at high velocities are present. Differential phase-contrast methods, however, which sense the first derivative of the phase, are highly sensitive to such smooth density gradients. Many of them are based on phase modulators and can be made compatible with single-shot acquisition. Among the many deterministic differential phase methods in the hard X-ray region, the most practical ones are based on periodic [6, 7] or random phase modulators [8, 9]. One of the most successful methods sensitive to density gradients is X-ray grating interferometry [10, 11], which has found broad application. The periodic phase gratings required for this method can be fabricated from low absorbing materials such as diamond with high precision [12] and can withstand the high photon fluence at XFEL sources. Several methods to obtain single-shot X-ray grating interferometry with a single phase grating have been demonstrated over the past years for high resolution phase microscopy and coherent probe characterisation [6, 7, 13, 14]. In this work, we combine multi-projection microscopy (in this case stereography) and single phase-grating interferometry to demonstrate, on a static phantom object, the feasibility of single-exposure, stereographic X-ray phase imaging. We propose that this method can be applied at megahertz XFEL sources where it will enable 4D (volume in time) visualisation of fast stochastic processes with enhanced constrast for the detection of smooth density gradients with sampling rates up to several MHz [15].

Our experiments were carried out at the Diamond Light Source (UK) high-coherence beamline I13-1 [16]. The photon energy was set to 12.6 keV using a horizontal two-bounce Si 111 monochromator. A linear diamond phase grating with pitch of 4 µm and structure height of 3.8 µm was placed in front of the thin Si 001 oriented crystal splitter. The diffraction vector of the phase grating was oriented in the vertical direction, perpendicular to the diffraction plane of the splitter, to avoid Fourier filtering of the diffracted waves from the grating. The splitter was a mono-crystalline membrane 30 µm thickness and with an effective area of 5 mm x 5 mm. It was produced in the laboratories of INFN-Ferrara (Italy) by anisotropic etching of a 500 µm thick wafer resulting in a thin membrane sustained by a frame. The main face and the sides have crystallographic orientations of (100), (010) and (001), respectively. X-rays passing through a mono-crystal generate a diffracted beam for each lattice plane positioned at the Bragg diffraction condition. The rules of symmetry for families of planes can be exploited for selecting multiple planes that diffract at the same Bragg angle for a specific photon energy to generate a plurality of virtually identical beams. The 113 family of planes was used in this experiment, and in particular the specular 113 and 1-1-3 planes. They present an asymmetry angle of 17.55° relative to the 100 direction (beam direction) and a rotation angle by 18.4° relative to the 001 direction. Therefore, the splitter was rotated of 18.4° around the optical axis so that the two diffracted beams remain in the horizontal diffraction plane (Fig. 1). The sample was placed just after the splitter in the beam overlap region, illuminating sample simultaneously by the two diffracted beams separated by an angle of 70.2°. The direct transmitted beam was not used

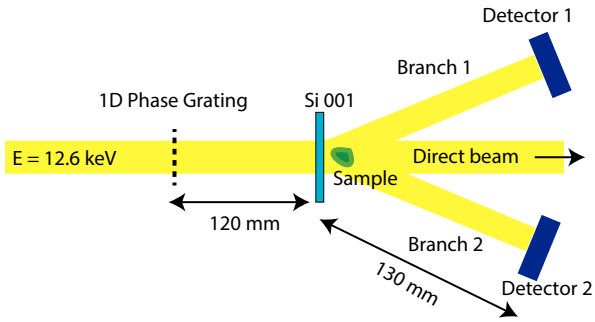


**Fig. 1.** Schematic representation of the proposed stereographic X-ray phase imaging method using a single phase grating made from diamond and a Si 001 crystal splitter. The crystal beam-splitter generates two identical X-ray beams using the 113 and 1-1-3 diffraction planes. The sample is placed in the overlap region of the beams just after the splitter and two self images are generated simultaneously at the position of two detectors, allowing for access to the phase gradient of the sample under two angular views. The angle between the two diffracted beams is 70.2°.

in this case. The sample consisted of soda lime glass spheres with a diameter of 100 µm glued onto a bundle of carbon fibres. Two simultaneous X-ray interferograms were generated at the imaging planes of the high-resolution X-ray microscopes. The projection interferometric images of the sample were simultaneously recorded by two high-resolution indirect-detection X-ray microscopes. Each microscope was composed of a scintillator coupled via a diffraction-limited optical microscope to a CCD detector (PCO4000, 4008 pixel × 2672 pixel, 9 µm pixel size). A total magnification of 20x was used in the experiment, providing an effective pixel size of 0.45 µm. An exposure time of 5s was used. Photograph of the experimental setup is shown in Fig. 2.

The recorded interferograms were processed using the Fourier method [17, 18] for extracting differential phase, followed by integration to obtain the phase maps. The results are shown in Fig. 3. The phase profiles obtained from the two branches match well with the theoretical phase profiles of lime glass spheres.

Further, we performed the 3D reconstruction of the sample using stereography point-based technique [19–21]. This method relies on identifying low-level primitives and points, and matching them on the multi-view images. As an example, it is possible to fit circles to the borders of the projections of the soda lime grass spheres, thus finding the positions of their centers. At this point, we can solve the problem with ray-tracing. We consider the beam parallel with $Z$ along the beam direction, $Y$ vertical (direction of gravity), $X$ horizontal, 1 and 2 being the two projections. With the beam parallel, we can solve the problem plane-by-plane, working on parallel $XZ$ planes and considering $Y$ identical for each corresponding sphere of the two projections $Y = Y1 = Y2$, except for a constant Y translation between the two images. We also know that the angles between the two projections is 70.2° and the inclination angle of the two projections with the direct beam ($Z$ direction) are 35.1° and -35.1°. This is also the inclination angle of the line that connects the centre of each projection to the corresponding centre of the sample sphere. The position of the sample sphere is the point where the two lines crossing each projection superimpose. The equations of the

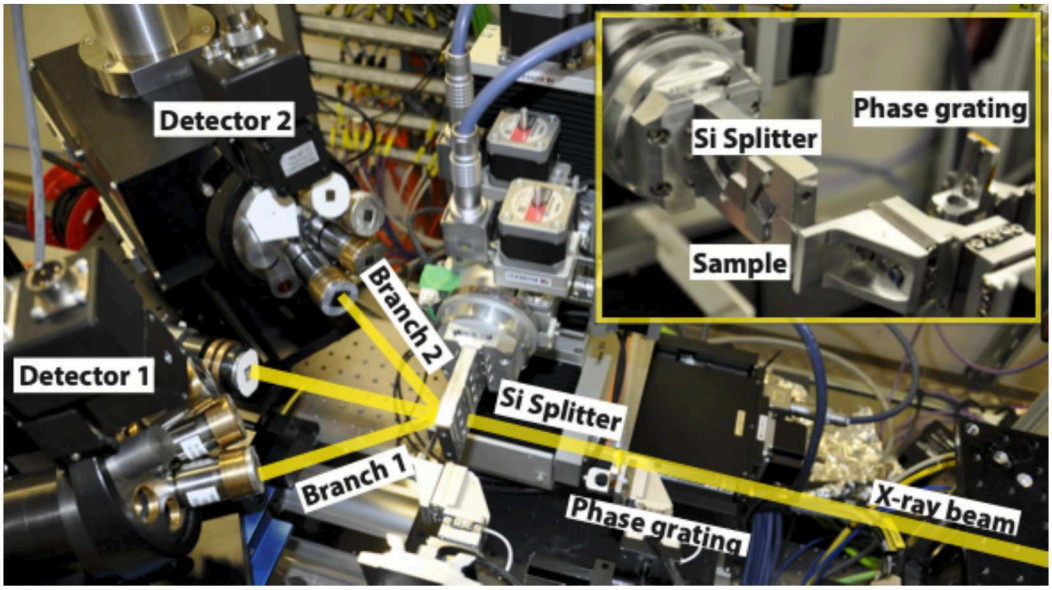


**Fig. 2.** Experimental configuration of the setup during the experiment at Diamond I13 coherence branch beamline. An overview of the entire setup with zoom on splitter and the sample, including the two detectors on the left and the beam splitter in the center.

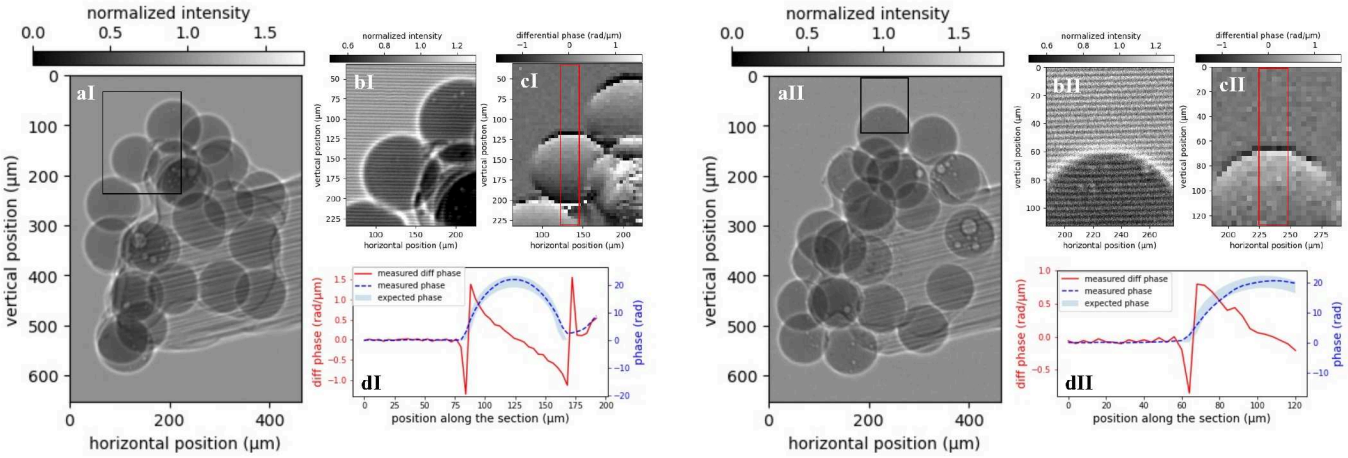


**Fig. 3.** (aI, aII) Absorption images for branch 1 and 2 obtained with the grating-based approach (bI, bII) Interferogram recorded for the black rectangle shown in panels (aI) and (aII), respectively for branch 1 (bI) and branch 2 (bII). (cI, cII) Differential phase reconstructed from the interferograms in the region of the black rectangle shown in panels (aI) and (aII), respectively for branch 1 (cI) and branch 2 (cII). (dI, dII) Comparison of the extracted differential phase, integrated phase and theoretically expected phase of the lime-glass spheres with a diameter of 100 µm including tolerance given by the manufacturer. The experimental plots represent an average over the columns in the red rectangles in panels (cI) and (cII).

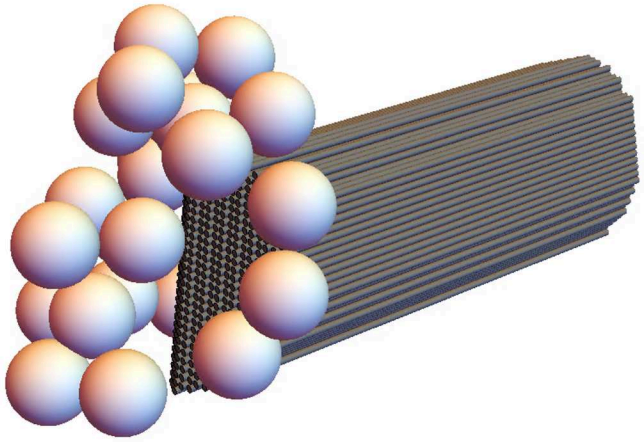

**Fig. 4.** 3D reconstruction of the sample achieved by stereography through point-based technique from the two stereographic projections at angles +35.1° and -35.1°. The soda-lime glass spheres are well distinguishable, as well as the structure of the carbon fibre thread, composed of a multitude of micrometric fibres.

lines are:

$$X_1 = k_1 \cdot Z_1 + X_{1o} \quad (1)$$
$$X_2 = k_2 \cdot Z_2 + X_{2o} \quad (2)$$

where $k_1 = 0.7028$ and $k_2 = -0.7028$ Naming $X_{P1}$ and $X_{P2}$ the $X$ positions of the centre of the projections of the sphere in the plane of the detector 1 and 2 respectively:

$$X_{1o} = X_{P1}/cos(angle) \quad (3)$$
$$X_{2o} = X_{P2}/cos(-angle) = X_2/cos(angle) \quad (4)$$

Thus we can solve the system of equation for their crossing point

$$X_1 = X_2 = X \quad (5)$$
$$Z_1 = Z_2 = Z \quad (6)$$
$$Z = (X_{2o} - X_{1o})/(k_1 - k_2) \quad (7)$$
$$X = X_1 = k_1 \cdot Z_1 + X_{1o} \quad (8)$$

The system is solved except for an $X$ and $Z$ translation. This system of equations can be applied to any point of the projections in order to attain the centres of all the soda lime glass spheres. The same procedure can be employed for the carbon fibres that holds the spheres by finding corresponding points in the two projections. The result is a weak solution of the system, which is usually the starting point for further refinement through the statistical methods, which was not performed in this work.

In summary, we have successfully demonstrated the combination of phase imaging using grating interferometry and stereographic image acquisition providing a single shot approach. From the simultaneously recorded interferograms, the phase information was recovered and the 3D information was accurately obtained as well. We propose the application of this method for stereographic or multi-projection microscopy at megahertz XFEL sources for the visualisation of phenomena such as liquid mixing or shock-wave propagation. It should be noted that the proposed method has limitations that need to be addressed and investigated in order to achieve a practical implementation at XFEL sources. The most significant is the photon energy acceptance of the splitter crystal, which limits the spectral bandwidth of the diffracted beams and can even lead to a fixed photon energy in case of multi-wave excitations. However, this issue could be removed by employing other splitter schemes that are tuneable in energy. Furthermore, the throughput of such devices can be optimised using, e.g. seeded SASE beams rather than a regular, SASE XFEL beam.

## FUNDING INFORMATION

The authors acknowledge funding support from Bundesministerium für Bildung und Forschung (BMBF) (05K18XXA); Vetenskapsrådet (VR) (2017-06719), Röntgen Ångström Cluster INVISION project

## ACKNOWLEDGMENTS

Beamtime was granted at Diamond Light Source beamline I13 in the frame of proposal MT17739.

## DATA AVAILABILITY STATEMENT

Data underlying the results presented in this paper are available upon request.

## FULL REFERENCES


1. M. Hoshino, K. Uesugi, J. Pearson, T. Sonobe, M. Shirai, and N. Yagi, "Development of an x-ray real-time stereo imaging technique using synchrotron radiation," J. Synchrotron Radiat. **18**, 569 – 574 (2011).
2. R. Mokso and P. Oberta, "Simultaneous dual-energy X-ray stereo imaging," J. Synchrotron Radiat. **22**, 1078–1082 (2015).
3. P. Villanueva-Perez, B. Pedrini, R. Mokso, P. Vagovic, V. A. Guzenko, S. J. Leake, P. R. Willmott, P. Oberta, C. David, H. N. Chapman, and M. Stampanoni, "Hard x-ray multi-projection imaging for single-shot approaches," Optica **5**, 1521–1524 (2018).
4. W. Voegeli, K. Kajiwara, H. Kudo, T. Shirasawa, X. Liang, and W. Yashiro, "Multibeam x-ray optical system for high-speed tomography," Optica **7**, 514–517 (2020).
5. F. García-Moreno, P. H. Kamm, T. R. Neu, F. Bülk, R. Mokso, C. M. Schlepütz, M. Stampanoni, and J. Banhart, "Using x-ray tomoscopy to explore the dynamics of foaming metal," Nat. Commun. **10**, 3762 (2019).
6. Y. Takeda, W. Yashiro, Y. Suzuki, S. Aoki, T. Hattori, and A. Momose, "X-ray phase imaging with single phase grating," Jpn. J. Appl. Phys. **46**, L89–L91 (2007).
7. W. Yashiro, Y. Takeda, A. Takeuchi, Y. Suzuki, and A. Momose, "Hard-x-ray phase-difference microscopy using a fresnel zone plate and a transmission grating," Phys. Rev. Lett. **103**, 180801 (2009).
8. S. Berujon, H. Wang, and K. Sawhney, "X-ray multimodal imaging using a random-phase object," Phys. Rev. A **86**, 063813 (2012).
9. K. S. Morgan, D. M. Paganin, and K. K. W. Siu, "X-ray phase imaging with a paper analyzer," Appl. Phys. Lett. **100**, 124102 (2012).
10. C. David, B. Nöhammer, H. H. Solak, and E. Ziegler, "Differential x-ray phase contrast imaging using a shearing interferometer," Appl. Phys. Lett. **81**, 3287–3289 (2002).
11. A. Momose, S. Kawamoto, I. Koyama, Y. Hamaishi, K. Takai, and Y. Suzuki, "Demonstration of x-ray talbot interferometry," Jpn. J. Appl. Phys. **42**, L866 (2003).
12. M. Makita, P. Karvinen, V. Guzenko, N. Kujala, P. Vagovic, and C. David, "Fabrication of diamond diffraction gratings for experiments with intense hard x-rays," Microelectron. Eng. **176**, 75 – 78 (2017). Micro- and Nano-Fabrication.
13. S. Matsuyama, H. Yokoyama, R. Fukui, Y. Kohmura, K. Tamasaku, M. Yabashi, W. Yashiro, A. Momose, T. Ishikawa, and K. Yamauchi, "Wavefront measurement for a hard-X-ray nanobeam using single-grating interferometry," Opt. Express **20**, 24977 (2012).
14. M. Seaberg, R. Cojocaru, S. Berujon, E. Ziegler, A. Jaggi, J. Krempasky, F. Seiboth, A. Aquila, Y. Liu, A. Sakdinawat, H. J. Lee, U. Flechsig, L. Patthey, F. Koch, G. Seniutinas, C. David, D. Zhu, L. Mikeš, M. Makita, T. Koyama, A. P. Mancuso, H. N. Chapman, and P. Vagovič, "Wavefront sensing at X-ray free-electron lasers," J. Synchrotron Radiat. **26**, 1115–1126 (2019).
15. P. Vagovič, T. Sato, L. Mikeš, G. Mills, R. Graceffa, F. Mattsson, P. Villanueva-Perez, A. Ershov, T. Faragó, J. Uličný, H. Kirkwood, R. Letrun, R. Mokso, M.-C. Zdora, M. P. Olbinado, A. Rack, T. Baumbach, J. Schulz, A. Meents, H. N. Chapman, and A. P. Mancuso, "Megahertz x-ray microscopy at x-ray free-electron laser and synchrotron sources," Optica **6**, 1106–1109 (2019).
16. C. Rau, S. Marathe, A. J. Bodey, M. Storm, D. Batey, S. Cipiccia, P. Li, and R. Ziesche, "Operando and high-throughput multiscale-tomography," in *Developments in X-Ray Tomography XIII,* vol. 11840 B. Müller and G. Wang, eds., International Society for Optics and Photonics (SPIE, 2021), pp. 192 – 200.
17. M. Takeda, H. Ina, and S. Kobayashi, "Fourier-transform method of fringe-pattern analysis for computer-based topography and interferometry," J. Opt. Soc. Am. **72**, 156–160 (1982).
18. H. H. Wen, E. E. Bennett, R. Kopace, A. F. Stein, and V. Pai, "Single-shot x-ray differential phase-contrast and diffraction imaging using two-dimensional transmission gratings," Opt. Lett. **35**, 1932–1934 (2010).
19. Y. Abdel-Aziz, H. Karara, and M. Hauck, "Direct linear transformation from comparator coordinates into object space coordinates in close-range photogrammetry*," Photogramm. Eng. Remote. Sens. **81**, 103–107 (2015).
20. L. H. André B, Dansereau J, "Effect of radiographic landmark identification errors on the accuracy of three-dimensional reconstruction of the human spine." Med. Biol. Eng. Comput. p. 569–575 (1992).
21. L. C. Chen, C. W. Armstrong, and D. D. Raftopoulos, "An investigation on the accuracy of three-dimensional space reconstruction using the direct linear transformation technique." J. biomechanics **27 4**, 493–500 (1994).